Biochimica et Biophysica Acta, 1140 (1992) 175–183

BBABIO 43723

Resonance Raman studies of Rieske-type proteins

Debasish Kuila [a,1], Jon R. Schoonover [a,2], R. Brian Dyer [a,3], Christopher J. Batie [b,4], David P. Ballou [b], James A. Fee [a] and William H. Woodruff [a]

[a] *Biochemistry and Spectroscopy Group, Isotope and Structural Chemistry Division, Los Alamos National Laboratory, Los Alamos, NM (USA) and* [b] *Department of Biological Chemistry, The University of Michigan, Ann Arbor, MI (USA)*

(Received 18 May 1992)

Key words: Iron-sulfur protein; Iron-sulfur cluster; Resonance Raman spectroscopy; Rieske-type cluster

Resonance Raman (RR) spectra are reported for the [2Fe-2S] Rieske protein from *Thermus thermophilus* (TRP) and phthalate dioxygenase from *Pseudomonas cepacia* (PDO) as a function of pH and excitation wavelength. Depolarization ratio measurements are presented for the RR spectra of spinach ferredoxin (SFD), TRP, and PDO at 74 K. By comparison with previously published RR spectra of SFD, we suggest reasonable assignments for the spectra of TRP and PDO. The spectra of PDO exhibit virtually no pH dependence, while significant changes are observed in TRP spectra upon raising the pH from 7.3 to 10.1. One band near 270 cm^{-1}, which consists of components at 266 cm^{-1} and 274 cm^{-1}, is attributed to Fe(III)-N(His) stretching motions. We suggest that these two components arise from conformers having a protonated-hydrogen-bonded imidazole (266 cm^{-1}) and deprotonated-hydrogen-bonded imidazolate (274 cm^{-1}) coordinated to the Fe/S cluster and that the relative populations of the two species are pH-dependent; a simple structural model is proposed to account for this behavior in the respiratory-type Rieske proteins. In addition, we have identified RR peaks associated with the bridging and terminal sulfur atoms of the Fe-S-N cluster. The RR excitation profiles of peaks associated with these atoms are indistinguishable from each other in TRP (pH 7.3) and PDO and differ greatly from those of [2Fe-2S] ferredoxins. The profiles are bimodal with maxima near 490 nm and > approx. 550 nm. By contrast, bands associated with the Fe-N stretch show a somewhat different enhancement profile. Upon reduction, RR peaks assigned to Fe-N vibrations are no longer observed, with the resulting spectrum being remarkably similar to that reported for reduced adrenodoxin. This indicates that only modes associated with Fe-S bonds are observed and supports the idea that the reducing electron resides on the iron atom coordinated to the two histidine residues. Taken as a whole, the data are consistent with an $S^t_2FeS^b_2Fe[N(His)]^t_2$ structure for the Rieske-type cluster.

Introduction

Proteins containing two Fe atoms and two inorganic S atoms in a [2Fe-2S] cluster are widely observed in nature, where they serve primarily as electron transfer agents [1,2]. At least four different classes of proteins that bind this cluster are known to exist. The first is the ferredoxins, which possess a nominally constant set of spectral properties and for which the Fe/S cluster is known to be coordinated to the protein by four cysteinyl S atoms [1–5]. Recently, the three-dimensional structures of ferredoxins from *Spirulina platensis* [4] and *Anabaena* [5] have been determined. Each contains a [2Fe-2S] cluster in which each Fe atom is coordinated by the two bridging sulfur atoms and by two cysteinyl sulfur atoms, i. e., $[Fe_2S^b_2]S^t(Cys)_4$ unit (S^b = bridging, S^t = terminal), and the coordination geometry at each Fe is roughly tetrahedral. Ferredoxins from other sources as well as synthetic analogs containing the [2Fe-2S] cluster have been widely characterized (cf. Refs. 1–3, 6, 7). The second class includes proteins such as adrenodoxin and putidaredoxin that have spectral properties distinct from the ferredoxins, but which nevertheless probably sequester the Fe/S cluster with cysteine residues [8,9]; their three-dimensional structures are not known. The third group is a new class of [2Fe-2S] containing proteins, discovered by Flint and Emptage [10]. These proteins have not yet been well characterized, but it has been suggested that non-sulfur atoms are coordinated to the [2Fe-2S] cluster. Finally,

Correspondence to: J.A. Fee, INC-14, MS C-345, LANL, Los Alamos, NM 87545, USA.

[1] Present address: Department of Physiology and Biophysics, Albert Einstein College of Medicine, Bronx, NY 10461, USA.

[2] Present address: Department of Chemistry, University of North Carolina, Chapel Hill, NC 27599, USA.

[3] Present address: Chemical and Laser Science Group, Los Alamos National Laboratory, Los Alamos, NM 87545, USA.

[4] Present address: Department of Biochemistry and Molecular Biology, Lousiana State University Medical Center, New Orleans, LA 70112, USA.

there are the so-called Rieske-type proteins (cf. Refs. 11–18 and references therein). Specific systems that have contributed to our knowledge of this class include the Rieske proteins from *Thermus thermophilus* (TRP) and *Rhodobacter capsulatus*, the mitochondrial Rieske protein, and phthalate dioxygenase (PDO) from *Pseudomonas cepacia*, as well as others.

The spectral and redox properties of Rieske-type centers are quite distinct from those of ferredoxins. Some notable differences include an average EPR *g*-value of 1.91 compared with 1.96 for the ferredoxins, a red-shifted, visible absorption with maximum absorptivity about 0.67 that of the ferredoxins, and very different circular dichroic spectra (cf. Ref. 11). The mid-point potentials of Rieske-type proteins are higher than ferredoxins and vary considerably within the group. The potentials of the respiratory-type proteins are unusually high, up to 350 mV, and linked to an ionization in the oxidized protein having a pK_a between 8 and 9, while those of Rieske-type dioxygenases are typically less than -100 mV and independent of pH. Ferredoxins have the lowest midpoint potentials (~ -400 mV), while putidaredoxin has a midpoint potential near -250 mV (cf. Refs. 11, 16 and references therein).

A combination of compositional and ENDOR studies of TRP, PDO and the cytochrome bc_1 complex from *R. capsulatus* and other organisms have shown that the [2Fe-2S] cluster in these proteins is coordinated by two histidines [13–15,18]. Preliminary RR results from our laboratories [17] suggested that the [2Fe-2S] clusters in TRP and PDO have C_{2v} symmetry, while Mössbauer studies of TRP [18] suggested that one Fe-atom of the cluster was coordinated to 4 S atoms, in both oxidized and reduced forms. These observations have led to a structural model in which 2 Cys coordinate one Fe while 2 His coordinate the other Fe, $S^t_2FeS^b_2Fe[N(His)]^t_2$; the model has been used to rationalize the above noted differences between ferredoxins and Rieske-type proteins (cf. Ref. 11).

Within this class of proteins there are significant differences, beginning with the nature of the protein moieties. TRP ($M_r \approx 20000$) appears to contain two identical [2Fe-2S] clusters in contrast to one [2Fe-2S] cluster in mitochondrial Rieske protein ($M_r \approx 24000$) and phthalate dioxygenase ($M_r \approx 48000$). Moreover, while the Fe/S cluster appears to be coordinated similarly in all cases, significant differences in spectral properties and chemical behavior indicate that the immediate environment of the cluster varies among the different proteins. Since RR spectroscopy has been extensively applied to [2Fe-2S]-containing ferredoxins (cf. Ref. 19 and references therein), we are utilizing this method to understand the similarities and differences between the Fe/S/N clusters of TRP and PDO and the Fe/S/S cluster of SFD. We present RR spectra of these systems in different states of protonation and reduction and as a function of excitation wavelength. The results are discussed in relation to previously reported data for various [2Fe-2S] proteins [19–25] and synthetic analogues [26,27].

Materials and Methods

The Rieske protein from *Thermus thermophilus* (TRP) was isolated by the method of Fee et al. with $A_{460}/A_{280} = 0.22$ [18]. The spinach ferredoxin (SFD) was purified by the procedure of Petering and Palmer [28]. The purity index of SFD was > 0.47 for all samples. The phthalate dioxygenase protein (PDO) from *Pseudomonas cepacia* was purified by the method of Batie et al. [29] with $A_{460}/A_{280} = 0.07$ for the isolated protein. Samples of SFD, TRP and PDO were prepared in Hepes at pH 7.3. The high-pH (pH 10.1) sample of TRP was buffered with CAPS ((3-cyclohexylamino)-1-propanesulfonic acid). All the samples used for RR spectroscopy were concentrated to an optical absorbance of about 1 per mm at 460 nm (about 1 mM in Fe/S). In all cases, samples were washed using an Amicon concentrator with several cycles in the desired buffer, and the final concentration was achieved by evaporation using a gentle flow of dry nitrogen. Highly luminesent RR samples were treated with charcoal to remove impurities, after which they were passed through a G-25 column equilibrated with the appropriate buffer. Samples used in the depolarization ratio measurements were concentrated to > 2 mM and diluted to 1 mM with ethylene glycol to give a 50% ethylene glycol solution; when frozen, these samples formed an optically clear glass. For the reduced protein studies, TRP and PDO were exposed to excess dithionite and immediately frozen for the RR measurements. Upon completion of the experiments, excess dithionite was removed using ultrafiltration and the purity index of the re-oxidized protein was checked, as were the samples of oxidized proteins.

RR spectra were obtained using a SPEX 1403 spectrometer equipped with a cooled RCA 31034 photomultiplier tube. Data acquisition was controlled by a MacIntosh II (Apple Computer). Laser excitation was provided by either a Spectra Physics 171-19 Ar^+ or 171-01 Kr^+ laser. A Coherent model 599 dye laser with Rhodamine 590 pumped by the Ar^+ laser was also used. Spectra were obtained using a scan rate of 1 cm^{-1} s^{-1} and a spectral resolution of 4 cm^{-1}. Raman scattering was collected in a 135° backscattering geometry off the surface of the frozen solution at nominal liquid nitrogen temperature (74 K, 0.82 atm). Laser power for all spectra was between 50 and 100 mW at the cryo window. Unless indicated otherwise, the spectra were not subjected to smoothing routines. All RR intensities were measured relative to the ice peak at 230 cm^{-1}.

Results and Discussion

Raman spectra

The resonance Raman (RR) spectra of the oxidized forms of SFD at pH 7.3, TRP at pH 7.3 and 10.1, and PDO at pH 7.3 are presented in Fig. 1. The principal RR frequencies of these systems at various excitation wavelengths are compared in Table I. With excitation into the strong visible absorption bands, which by comparison to other Fe-S proteins are presumed to be associated with S ⇒ Fe charge-transfer transitions, the RR spectra between 100 and 450 cm^{-1} are expected to be dominated by Fe-S vibrational modes. With the Rieske proteins, one might also expect to observe Fe-N vibrational modes. The spectrum of SFD is nearly identical to the spectrum of ferredoxin from *Spirulina platensis* which has a known crystal structure [23,25]; this structure is thus useful in interpreting the data for SFD *. SFD has been extensively studied by RR spectroscopy and assignments have been made using comparisons with [2Fe-2S] model complexes, isotopic substitution, excitation profiles and normal coordinate analysis [19–27].

The assignments in ferredoxins and by inference the Rieske protein are complicated by the fact that the Fe-S^t-C and cysteine S^t-C-C angle bending vibrations are expected in the region of observation, and these may mix with vibrations of the $[Fe_2S_2^b]S^t(Cys)_4$ core. We demonstrated this effect in studies of blue copper proteins, which showed that internal ligand deformations can have a substantial effect on the RR spectra of the chromophore [30]. This was subsequently confirmed for the particular case of Fe/S proteins by Han et al. [26] who demonstrated interaction between the S^t-C-C bending motion and two Fe-S^t stretching modes, as well as substantial coupling between terminal and bridging Fe-S modes in [2Fe-2S] protein analogues. This mixing is dependent upon the Fe-S^t-CC dihedral angle, which varies in the different [2Fe-2S] proteins. Additionally, hydrogen bonding interactions can have an appreciable effect on the frequencies of the Fe-S vibrations in different proteins [23].

As shown in Table I, ferredoxin RR spectra exhibit seven well documented RR lines. By contrast to the ferredoxin spectra, the RR spectra of TRP and PDO show at least ten peaks below 450 cm^{-1}, depending on excitation wavelength (see Fig. 1). As discussed previously [17], the appearance of more peaks in the PDO and TRP spectra can be understood by comparing the symmetry of the $[Fe_2S_2^b]S^t(Cys)_4$ core to the structural

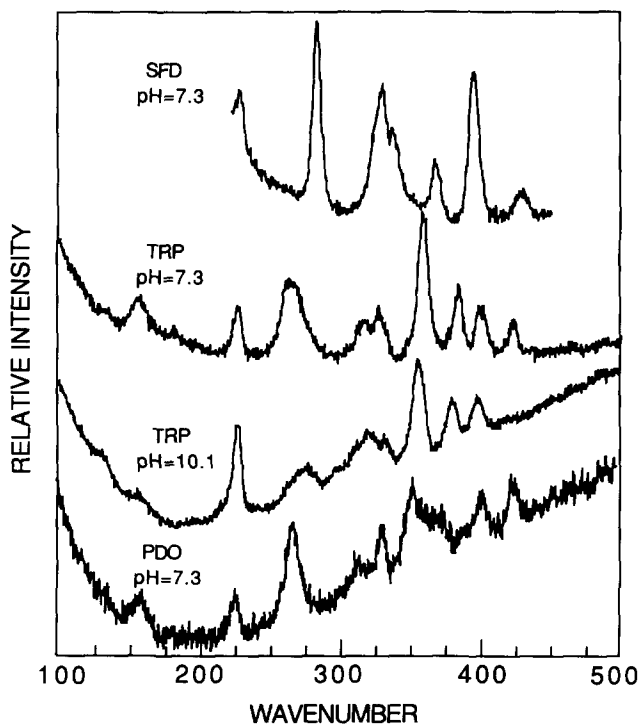

Fig. 1. Resonance Raman (RR) spectra between 100 and 450 cm^{-1} of oxidized samples of SFD at pH 7.3, TRP at pH 7.3, TRP at pH 10.1 and PDO at pH 7.3. Excitation wavelengths were 457.9 nm for SFD, 568.3 nm for PDO and TRP at pH 7.3 and 488.0 nm for TRP at pH 10.1. The spectra were obtained at 74 K in a 135° backscattering geometry with laser power between 50 and 100 mW at the cryowindow. The scan rate was 1 cm^{-1} s^{-1} with a spectral resolution of 4 cm^{-1}. The optical absorbance for the protein samples was > 1/mm at 460 nm (i.e., concentration > 1 mM).

TABLE I

Comparison of resonance Raman peaks (250–450 cm^{-1}) for Thermus Rieske protein (TRP), Pseudomonas phthalate dioxygenase (PDO), and ferredoxins from Spinacea aleracea (SFD) and Porphyra umbilicalis (PUF)

Mode [b]	TRP		PDO [a]	SFD [a]	PUF [a]
	pH 7.3	pH 10.1			
Fe-N^t	266	266 sh[i]	–	–	
Fe-N^t	274 w,sh	274	–	–	
Fe-S^t	–	–	–	283	282
Fe-N^t	–	300	–	–	–
Fe-S^t	322	322	315	–	–
Fe-S^b	330	330	334	329	329
Fe-S^t	–	–	–	336	339
Fe-S^t	360	357	354	350 w	357
Fe-S^t	–	–	372	–	–
Fe-S^b	–	–	–	366	367
Fe-S^b	384	382	390 sh	394	395
Fe-S^b	402	400	404	–	–
Fe-S^b	424	424 w	426	428	426

[a] pH 7.3.

[b] Superscript t indicates a terminal ligand and superscript b indicates a bridging ligand. [i]sh indicates the presence of a shoulder, w signifies a weak Raman line. TRP and PDO data from this work; SFD and PUF data from Ref. 19.

* It should be noted, however, that subtle differences were found in the spectra of these two ferredoxins in the presence of D_2O, probably due to different hydrogen bonding effects [22]. We assume nevertheless that the structures are fundamentally similar.

options of the iron-sulfur-nitrogen clusters. In the centrosymmetric structures (point groups D_{2h} and C_{2h}) possible for the $[Fe_2S_2^b]S^tN^t$ core of the Rieske-type proteins (and discounting possible contributions from skeletal modes of the ligands) there are nine Raman active vibrations. Accordingly, with the peaks observed in the TRP and PDO spectra, the symmetry of the $[Fe_2S_2^b]S^t(Cys)_2N(His)_2$ cluster is likely not centrosymmetric. We therefore concluded [17] that the structure must be at most C_{2v} with either one nitrogen on both irons or both nitrogens on one iron. The latter structure is preferred, since the observed number of peaks can occur only if the iron-sulfur core experiences a major perturbation away from centrosymmetry such that formerly ungerade motions become Raman allowed; and, this structure is supported by Mössbauer studies of TRP [18].

Fig. 1 illustrates some of the strong similarities between the RR spectra of SFD, TRP, and PDO. In contrast to the established spectrum of various ferredoxins, TRP and PDO show additional peaks between 200 and 330 cm^{-1}, some of which presumably possess substantial Fe(III)-N(His) character. TRP and PDO are expected to exhibit Fe(III)-N stretches in addition to the vibrations observed in the purely iron-sulfur proteins and these peaks are expected in the 200 to 300 cm^{-1} region (cf. Refs. 31–33).

In comparing the observed Raman peaks between 250 and 450 cm^{-1} (see Table I) with ferredoxins, additional peaks are clearly observed near 260 and 400 cm^{-1} for TRP and PDO. At least two more peaks are observed between 300 and 350 cm^{-1}, but exact frequencies are difficult to assign because this region is unresolved. Indeed, some of the Raman peaks in TRP and PDO are weak and only definitively observed at certain excitation wavelengths. It should further be noted that comparisons to spectra of ferredoxins are difficult in the absence of isotope data. Below 200 cm^{-1} where angle deformations are expected, at least one additional peak is evident in TRP and PDO as compared to SFD (not shown here). Bending motions such as S-Fe-S and Fe-S-Fe are expected for SFD, while TRP and PDO should exhibit these deformations as well as motions involving the nitrogen ligands.

Overtone and combination modes have been observed in the 500–800 cm^{-1} region for several [2Fe-2S] ferredoxins [20,22,25]. However, no such lines are observed in the spectra of TRP and PDO (spectra not shown).

Depolarization ratio measurements

Depolarization ratios can provide information about the symmetry of the various vibrational modes. Spectra were recorded at low temperature (74 K) in a 1:1 ethylene glycol/water glass, and depolarization ratios measured for several RR peaks of SFD, TRP and PDO at pH 7.3 (Table II). In agreement with the results of Meyer et al. [22], we find three and possibly five peaks in the spectrum of SFD to be polarized and therefore due to symmetric vibrations. The Raman peaks at 283, 328 and 394 cm^{-1} are clearly polarized. In addition, the peaks at 336 and 366 cm^{-1}, appear to be polarized, but this conclusion must be tempered somewhat due to experimental uncertainty in the intensity measurements. The remaining peaks are not of sufficient intensity to determine their depolarization ratios.

TABLE II

Resonance Raman frequencies (cm^{-1}) and depolarization ratios [a] measured for TRP, PDO and SFD at pH 7.3

TRP	PDO	SFD [b]	SFD [c]
266\0.49 p		283\0.48 p	285\0.46 p
330\0.36 p	334\0.38 p	328\0.48 p	330\0.40 p
		336\0.57 p or d	340\0.50 p or d
359\0.58 p or d	354\0.34 p		
	372\0.30 p	366\0.55 p or d	369\0.55 p or d
384\0.38 p		394\0.48 p	397\0.38 p
401\0.33 p	404\0.43 p		
424\0.18 p	426\0.35 p		428\0.53 p or d

[a] Data obtained in a glass of 1:1 ethylene glycol to water at 74 K. p indicates polarized and d represents depolarized; estimated error is ± 20%.
[b] This work.
[c] From Ref. 22.

Depolarization ratio measurements of TRP and PDO indicate that at least five of the observed Raman peaks are polarized. In TRP the peaks at 266, 330, 384, 402 and 424 cm^{-1} are due to polarized vibrations. The Raman peak at 360 cm^{-1} may be polarized, while the remaining peaks are of insufficient intensity to obtain accurate measurements. The PDO peaks which are definitely polarized are located at 334, 354, 372, 404, and 426 cm^{-1}. Depolarization ratios above about 0.3 for all modes provide clear indication that the core in TRP and PDO has an effective symmetry lower than the idealized maximum symmetry of C_{2v} (cf. Ref. 22).

pH effects

The [2Fe-2S] cluster of PDO appears to be structurally similar to those of the TRP, but there are some significant differences. As noted above, the midpoint potentials of PDO and related dioxygenases are typically less than −100 mV, while the midpoint potentials of the clusters in Rieske proteins are above 100 mV. The potentials in the Rieske proteins are affected by a redox-linked protonation of the cluster wherein the oxidized form of the cluster reversibly loses a proton

with $pK_a \approx 8$ (cf. Ref. 11). We previously reported that the relative RR intensities and some frequencies in the spectrum of TRP appeared to be pH-dependent [17]. These changes are not observed in spectra of PDO or SFD. To differentiate between the effect of pH on RR frequencies and on changes in resonance enhancement at different pH values in TRP, the RR spectra of TRP at pH 7.3 and 10.1 were compared to that of PDO as a function of excitation wavelength (Figs. 2–5). The optical spectrum, certain RR frequencies, and the RR excitation profile of TRP at pH 10.1 are markedly different from those of the protein at pH 7.3. Fig. 2 shows the optical spectra of TRP at pH 7.3 and 10.1 along with the excitation profiles for the more intense RR peaks. Figs. 3, 4 and 5 present the RR spectra of TRP at pH 7.3, TRP at pH 10.1 and PDO at pH 7.3, respectively, as a function of excitation wavelength.

The TRP RR spectra reveal several changes upon raising the pH from 7.3 to 10.1. The peak at 266 cm^{-1} at pH 7.3 shifts at the higher pH to 274 cm^{-1}. The very slight asymmetry of the 266 cm^{-1} peak at pH 7.3 may be due to the presence of a 274 cm^{-1} peak as a weak shoulder. A shoulder at 266 cm^{-1} is discernable on the 274 cm^{-1} peak in the pH 10.1 spectrum, suggesting the presence of an additional peak near 270 cm^{-1}. Excitation profile data (Figs. 3 and 4) indicate that this intensity change is not a result of differing resonance enhancement arising from changes in the absorption

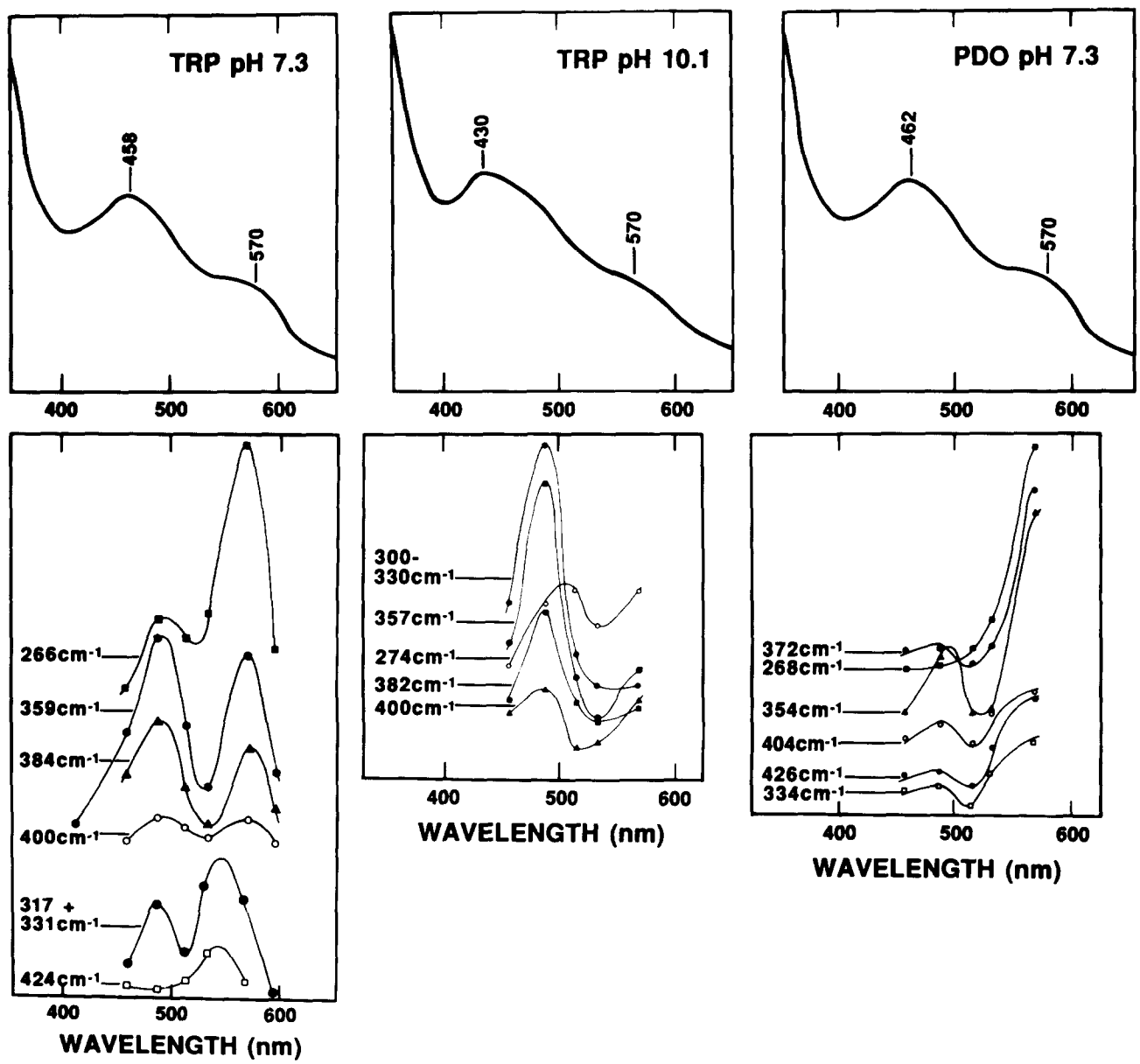

Fig. 2. The optical spectra (top panels) and Raman excitation profiles for individual Raman modes (bottom panels) are presented for PDO and TRP at pH 7.3 and TRP at pH 10.1. The intensities for the excitation profile are relative to the ice peak at 230 cm^{-1}. The actual spectra are displayed in Figs. 3, 4 and 5.

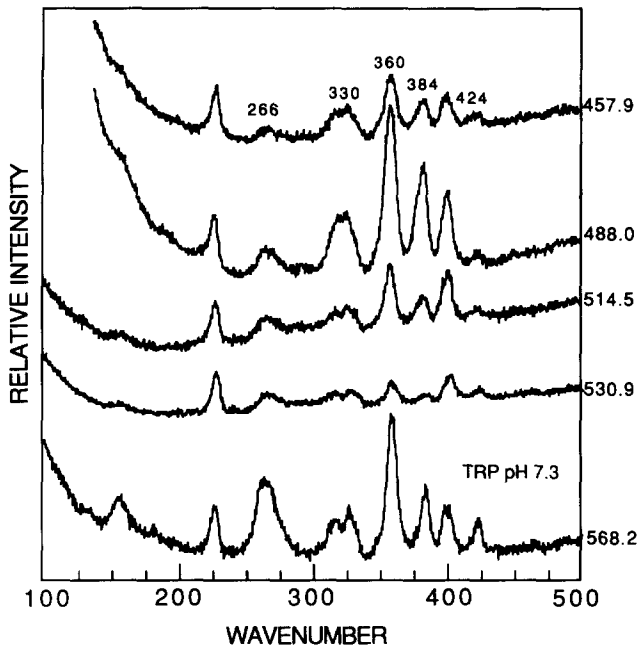

Fig. 3. RR spectra of oxidized TRP at pH 7.3 as a function of laser excitation wavelength. The spectra were obtained with the laser wavelength noted to the right of the spectrum with the conditions as in Fig. 1.

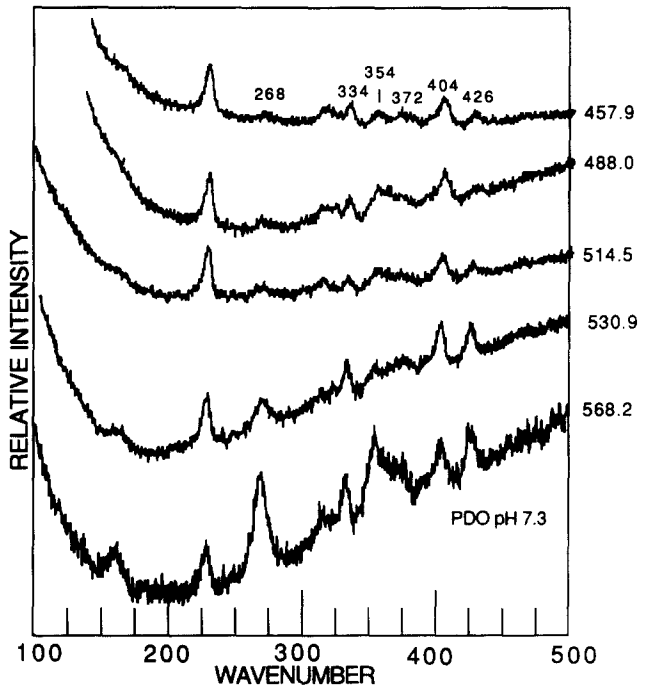

Fig. 5. RR spectra of oxidized PDO at pH 7.3 as a function of excitation wavelength; conditions as in Fig. 1 with the wavelength listed to the right of the spectrum.

spectrum. The 274-cm^{-1} peak gains intensity at pH 10.1 with a concomitant loss in intensity at 266-cm^{-1}; this is independent of excitation wavelength. We suggest that these peaks are predominately Fe(III)-N(His) in character, and exhibit the observed pH-dependent shift because of protonation and deprotonation of one of the Fe-bound histidine imidazoles (Ref. 34; cf. Ref. 11 and below). The small shift in vibrational frequency is consistent with the protonated form possessing a hydrogen bond. For example, the Fe(II)-N(His) frequency in cytochrome *c* peroxidase consists of components at 233 cm^{-1} and 246 cm^{-1} assigned to hydrogen bonded and deprotonated imidazole, respectively, while, in the non-hydrogen bonded form, the Fe(II)-N(His) is observed at 205 cm^{-1} [35]. Additionally, a Raman band appears at 300 cm^{-1} in the TRP spectrum at pH 10.1. This peak is likely shifted from the 300–320 cm^{-1} region, although it is difficult to quantify this shift because this region of the spectrum contains numerous overlapping peaks. In idealized C_{2v} symmetry for the $[S^t_2FeS^b_2Fe[N(His)]^t_2]$ cluster, two Fe-N^t stretches are Raman active, making it likely that the band at 300 cm^{-1} in the pH 10.1 TRP sample is due to an Fe-N^t stretch.

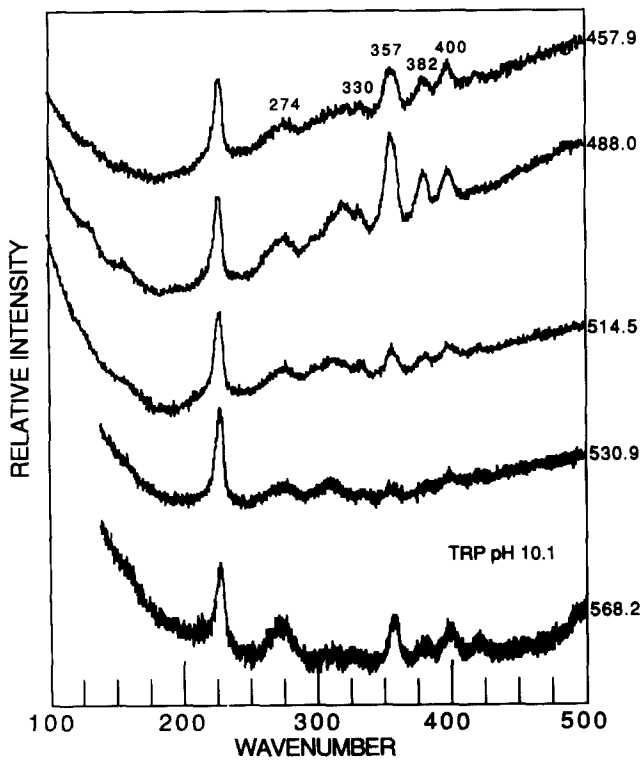

Fig. 4. RR spectra of TRP at pH 10.1 at various excitation wavelengths. The conditions are as in Fig. 1 and the laser wavelength is to the right of the spectrum.

The structural change need not be localized to one or two vibrational modes, nor will the pH dependence necessarily follow a simple equilibrium. Indeed, RR peaks other than the 266–274 cm^{-1} pair undergo frequency shifts with changing pH. The peaks at 402, 384 and 360 cm^{-1} shift to 400, 382 and 357 cm^{-1}, respectively, upon raising the pH. These peaks are probably Fe-S vibrations, the frequency shifts reflecting the effect of deprotonation upon Fe-S bonding. This slight

weakening of the Fe-S bonds is either caused directly by the strengthening of the Fe-N bond upon deprotonation or by a protein conformational change which may accompany the protonation/deprotonation reaction. There may be additional changes in the 300 to 350 cm^{-1} range, but these are difficult to gauge because of the numerous overlapping Raman lines. Another change observed at high pH is the loss of intensity of the RR peak at 424 cm^{-1}. At pH 10.1 the 424 cm^{-1} peak appears very weak with exciting wavelengths between 457.9 and 530.9 nm, but it gains intensity with 568.2 nm excitation (see Fig. 4). Accordingly, the intensity change in this peak can be ascribed to changes in resonance enhancement (see below).

It has previously been suggested that ionization of one of the coordinated histidine imidazole groups is responsible for the pH dependence of E_m observed with the respiratory-type proteins [11,16]. This is reasonable because coordination to a metal is known to strongly shift the pK_a of the imidazole/imidazolate equilibrium toward lower pH (from $pK_a = 14.2$) (cf. Ref. 36 and references therein). Moreover, the present RR data are generally consistent with such an ionization occurring between pH 7.3 and 10.1. The most likely explanation for the fact that the two bands (266 cm^{-1} dominant at pH 7.3 and 274 cm^{-1} dominant at pH 10.1) are both observed at the pH extremes is that only one of the two imidazole rings ionizes at high pH. That is, the shoulder on the high-wavenumber side of the 266 cm^{-1} peak is likely caused by a small amount of ionization at pH 7.3. At pH 10.1, the shoulder near 266 cm^{-1} represents the mode for the second imidazole ring which does not ionize, much the same as PDO. Previous measurements suggested $pK_a \approx 8$ [15], but unpublished work indicates that this value may depend on the preparation of TRP *. Because PDO appears to be insensitive to changes in pH, it would seem that the coordination effect by itself is not adequate to shift the ionization of the coordinated imidazole into our working pH range. To account for this difference in behavior between the two proteins, we speculate that an additional aid to ionization must exist in the respiratory-type proteins, namely a closely disposed, positively charged amino acid residue that could form a hydrogen bond with the coordinated imidazolate. The presence of a nearby positive charge could have the additional effect of stabilizing the reduced form, thereby raising the mid-point potential.

Wavelength dependence

The visible absorption spectra of the Rieske-type proteins contain numerous overlapping, broad bands due to ligand-to-metal charge-transfer transitions. The optical spectra of TRP and PDO at pH 7.3 (Fig. 2) exhibit absorbance maxima near 570 and 460 nm, while the spectrum of TRP at pH 10.1 demonstrates some differences. The excitation profiles of the stronger RR peaks are shown in the lower panel in Fig. 2. The ice band at 230 cm^{-1} served as the internal intensity standard.

Yachandra et al. [20] noted a different degree of resonance enhancement for bridging versus terminal sulfur modes of SFD, and Willis and Loehr [37] also observed this type of behavior for [2Fe-2S] centers from milk xanthine oxidase. No differential enhancement of Fe-S^t and Fe-S^b modes is evident in the spectra of TRP and PDO. However, the Raman peak at 266 cm^{-1} in TRP at pH 7.3 (274 cm^{-1} at pH 10.1), which we assign as substantially Fe(III)-N(His) in nature, shows a unique excitation profile when compared to the other Raman lines (Fig. 2). It is also significant that the 268-cm^{-1} peak in PDO spectra is the only Raman line which shows little wavelength dependence between 450 and 500 nm. This observation suggests the possibility that the 268-cm^{-1} peak, like the mode near 270 cm^{-1} in TRP, is due to a Fe(III)-N(His) stretch. The excitation profiles of TRP and PDO differ significantly from what is expected considering the similarity of their absorption spectra. For example, the excitation profile of adrenodoxin [19] roughly tracks the absorption spectrum, with greater enhancement occurring with shorter excitation wavelength. In contrast, TRP and PDO demonstrate remarkable enhancements at longer wavelengths. The TRP and PDO profiles show a maximum near 490 nm and another at longer wavelength (> about 550 nm). Interference effects from the different charge transfer transitions and anti-resonance effects may be important in causing these unique profiles.

Reduced TRP and PDO

RR spectra of reduced ferredoxins have to our knowledge, not previously been reported (cf. Ref. 38). Several papers [19,23,25] have, however, reported spectra of reduced adrenodoxin and 'red paramagnetic protein' (RPP) from *Clostridrium pasteurianum*. The data were interpreted as showing that the added electron is localized on one end of the $[Fe_2S_2^b]S^t(Cys)_4$ unit such that the core is $[Fe(II)S_2^bFe(III)]$. Upon reduction, the frequencies of bridging modes shift to lower frequency by 15–24 cm^{-1} due to a weakening of the bridge bonds to the Fe(II) side of the cluster. In adrenodoxin, the assignments of the Fe-S^b vibrations were confirmed by frequency shifts upon isotopic substitution of the bridging S atoms [19].

Fig. 6 presents the RR spectra of reduced PDO and TRP. As in adrenodoxin and RPP, the peaks believed

* Unpublished circular dichroism spectra obtained in the pH range 7 to 10 suggest a pK_a of about 9 (Kuila, D., Edmondson, S. and Fee, J.A. unpublished data).

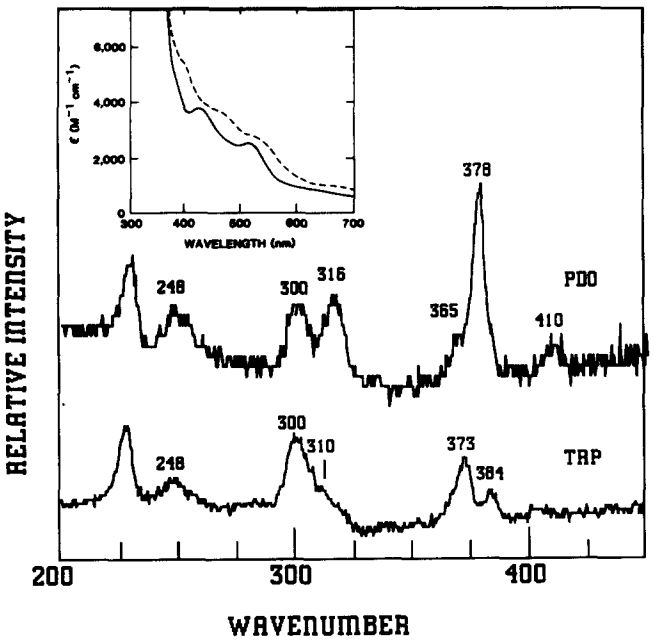

Fig. 6. RR spectra of dithionite-reduced PDO (top trace) and TRP (bottom trace) between 200 and 450 cm^{-1}. Both spectra were recorded at 74 K using 514.5 nm excitation and the instrumental conditions noted in Fig. 1. Because the S/N was significantly lower (cf. Ref. 38), these spectra have been subjected to a smoothing routine. The inset provides the optical spectra of reduced SFD (dashed) and TRP (solid) (cf. Ref. 11); the optical spectra of reduced TRP and PDO are indistinguishable.

to be primarily Fe-S^b stretching modes exhibit a significant shift to lower frequency. In TRP, the peaks in the oxidized protein at 384 and 402 cm^{-1} ascribed to Fe-S^b motions shift to 373 and 384 cm^{-1} in the reduced form. Likewise, the 404 cm^{-1} band in oxidized PDO and the accompanying shoulder at 390 cm^{-1} shift to 378 and 365 cm^{-1}. The other Raman peaks in the oxidized proteins attributed to $Fe_2S_2^b$ stretches are at 426 (PDO) and 424 cm^{-1} (TRP) and shift to 410 and 405 cm^{-1}, respectively, in the reduced spectra.

There are three additional peaks in the reduced protein spectra of PDO and TRP between 200 and 320 cm^{-1} which are similar to those reported for adrenodoxin and RPP. A straightforward explanation for this close similarity for Fe/S and Fe/S/N clusters in the reduced state is that the observed peaks in these spectra arise from either Fe-S^b or Fe-S^t modes of the Fe(III) side of the cluster. It appears that in the RR spectra of the reduced proteins, the Fe(III)-S vibrations are selectively enhanced over the Fe(II)-S (or N) modes, which are not observed in either the Fe-S or the Fe-S-N clusters. The foregoing suggests that the electron in reduced TRP and PDO resides at the Fe atom bound by the two imidazole nitrogens from the histidine residues.

Conclusions

RR spectra have been assigned for a class of [2Fe-2S] proteins that contain histidine-imidazole in addition to sulfur ligands. The Fe-S^t and Fe-S^b modes in TRP and PDO have been identified by comparison with the well-established spectrum of SFD. These assignments are verified with the spectra of reduced TRP and PDO as the Fe-S^b modes exhibit the expected shift to lower frequency upon reduction. Excitation profile data demonstrate that the Fe-N modes are enhanced in a different manner than the Fe-S^t or Fe-S^b modes.

The Raman spectrum of TRP, but not that of PDO, is sensitive to pH. Varying the pH permitted the assignment of a RR band near 270 cm^{-1} to an Fe(III)-N(His) stretch. It is suggested that this band consists of two components arising from populations having protonated-hydrogen-bonded imidazole and deprotonated-hydrogen-bonded imidazolate. This protonation/deprotonation equilibrium of an Fe/S coordinated imidazole ring is proposed to be responsible for the pH dependence of E_m, and a simple structural model involving the formation of an Fe bound imidazolate group near a positively charged residue is proposed to distinguish the pH-dependent behavior of TRP and PDO.

Raman spectra of reduced TRP and PDO are very similar to those published for adrenodoxin and RPP [19,23,25]. This result demonstrates that only Fe(III)-S modes are observed and is consistent with the idea that in Rieske-type proteins the electron resides on the iron atom bound by the histidine residues. The reduced protein spectra thereby supply additional evidence for the proposed structure of the $[Fe_2S_2^b]S^t(Cys)_2N(His)_2$ unit where the two histidine residues are bound to the same iron atom.

Acknowledgements

This work was supported by U.S. Public Health Service NIH Grants GM35342 to J.A.F., DK36263 to W.H.W and GM20877 to D.P.B. The work performed at Los Alamos National Laboratory was carried out under the auspices of the U.S. Department of Energy.

References

1 Beinert, H. (1990) FASEB J. 4, 2483–2491.
2 Spiro, T.G. (ed.) (1982) Iron-Sulfur Proteins, Wiley-Interscience, New York.
3 Matsubara, H., Katsube, Y. and Wada, K. (eds.) (1987) Iron-Sulfur Protein Research, Springer, Berlin.
4 Fukuyama, K., Hase, T., Matsumoto, S., Tsukihara, T., Katsube, Y., Tanaka, N., Kakudo, M., Wada, K. and Matsubara, H. (1980) Nature 286, 522–524.
5 Rypniewski, W.R., Breiter, D.R., Benning, M.W., Wesenberg, G., Oh, B.-H., Markley, J.L., Rayment, I. and Holden, H. (1991) Biochemistry 30, 4126–4131.

6 Bearwood, P. and Gibson, J.F. (1983) J. Chem. Soc. Dalton Trans., 737–748.
7 Sands, R.H. and Dunham, W.R. (1975) Q. Rev. Biophys. 7, 443–504.
8 Estabrook, R.W., Simpson, K., Mason, J.I., Baron, J., Taylor, W.E., Simpson, E.R., Purvis, J. and McCarthy, J. (1973) in Iron-Sulfur Proteins (Lovenberg, W. ed.), Vol. I, Ch. 8, pp. 193–223, Academic Press, New York.
9 Gunsalus, I.C. and Lipscomb, J.D. (1973) in Iron-Sulfur Proteins (Lovenberg, W., ed.), Vol. I, Ch. 6, pp. 151–171, Academic Press, New York.
10 Flint, D.H. and Emptage, M.H. (1988) J. Biol. Chem. 263, 3558–3564.
11 Fee, J.A., Kuila, D., Mather, M. and Yoshida, T. (1986) Biochim. Biophys. Acta 853, 153–185.
12 Batie, C.J., Ballou, D.P. and Correll, C.C. (1991) in Chemistry and Biochemistry of Flavoproteins, (Müller, F., ed.), Vol. 3, Ch. 18, CRC Press, Boca Raton.
13 Gurbiel, R.J., Batie, C.J., Sivaraja, M., True, A.E., Fee, J.A., Hoffman, B.M. and Ballou, D.P. (1989) Biochemistry 28, 4861–4871.
14 Britt, R.D., Sauer, K., Klein, M.P., Knaff, D.B., Kriauciunas, A., Yu, C.-A., Yu, L. and Malkin, R. (1991) Biochemistry 30, 1892–1901.
15 Gurbiel, R.J., Ohnishi, T., Robertson, D.E., Daldal, F. and Hoffman, B.M. (1991) Biochemistry, 30, 11579–11584.
16 Kuila, D. and Fee, J.A. (1986) J. Biol. Chem. 261, 2768–2771.
17 Kuila, D., Fee, J.A., Schoonover, J.R., Woodruff, W.H., Batie, C.J. and Ballou, D.P. (1987) J. Am. Chem. Soc. 109, 1559–1561.
18 Fee, J.A., Findling, K.L., Yoshida, T., Hille, R., Tarr, G.E., Hearshen, D.O., Dunham, W.R., Day, E.P., Kent, T.A. and Münck, E. (1984) J. Biol. Chem. 259, 124–133.
19 Han, S., Czernuszewicz, R.S., Kimura, T., Adams, M.W.W. and Spiro, T.G. (1989) J. Am. Chem. Soc. 111, 3505–3511.
20 Yachandra, V.K., Hare, J., Gewirth, A., Czernuszewicz, R.S, Kimura, T., Holm, R.H. and Spiro, T.G. (1983) J. Am. Chem. Soc. 105, 6462–6468.
21 Meyer, J., Moulis, J.-M. and Lutz, M. (1984) Biochem. Biophys. Res. Commun. 119, 828–835.
22 Meyer, J., Moulis, J.-M. and Lutz, M. (1986) Biochim. Biophys. Acta. 873, 108–118.
23 Mino, Y., Loehr, T.M., Wada, K., Matsubara, H. and Sanders-Loehr, J. (1987) Biochemistry 26, 8059–8065.
24 Spiro, T.G., Czernuszewicz, R.S. and Han, S. (1988) in Biological Applications of Raman Spectroscopy (Spiro, T.G. ed.), Vol. III, Ch. 12, pp. 523–553, Wiley & Sons, New York.
25 Yachandra, V.K., Hare, J., Gewirth, A., Czernuszewicz, R.S., Kimura, T., Holm, R.H. and Spiro, T.G. (1983) J. Am. Chem. Soc. 105, 6462–6468.
26 Han, S., Czernuszewicz, R.S. and Spiro, T.G. (1989) J. Am. Chem. Soc. 111, 3496–3504.
27 Bearwood, P. and Gibson, J.F. (1984) J. Chem. Soc. Dalton Trans. 1507–1516.
28 Petering, D.H. and Palmer, G. (1970) Arch. Biochem. Biophys. 141, 456–464.
29 Batie, C., LaHaie, E. and Ballou, D.P. (1987) J. Biol. Chem. 262, 1510–1518.
30 Blair, D.F., Campbell, G.W., Schoonover, J.R., Chan, S.I., Gray, H.B., Malmstrom, B.G., Pecht, I., Swanson, B.I., Woodruff, W.H., Cho, W.K., English, A.M., Fry, H.A., Lum, V. and Norton, K.A. (1985) J. Am. Chem. Soc. 107, 5755–5766.
31 Kurtz, D.M., Shriver, D.F. and Klotz, I.M. (1977) Coord. Chem. Rev. 24, 145–178.
32 Felton, R.H., Barrow, W.L., May, S.W., Sowell, A.L., Goel, S., Bunker, G and Stern, E.A. (1982) J. Am. Chem. Soc. 104, 6132–6134.
33 Walters, M.A. ad Spiro, T.G. (1983) Inorg. Chem. 22, 4014–4017.
34 Kitagawa, T. (1988) in Biological Applications of Raman Spectroscopy (Spiro, T.G., (ed.), Vol. III, Ch. 3, pp. 97–131, Wiley & Sons, New York.
35 Smulevich, G., Mauro, J.M., Fishel, L.A., English, A.M., Kraut, J. and Spiro, T.G. (1988) Biochemistry 27, 5477–5485.
36 Winter, J.A., Caruso, D. and Shepard, R.E. (1988) Inorg. Chem. 27, 1086–1089.
37 Willis, L.J. and Loehr, T.M. (1985) Biochemistry 24, 2768–2772.
38 Macor, K.A., Czernuszewicz, R.S., Adams, M.W.W. and Spiro, T.G. (1987) J. Biol. Chem. 262, 9945–9947.